

- M. E. Schwab, *Mamm. Genome* **5**, 180 (1994).
15. C. Le Moine and W. S. Young III, *Proc. Natl. Acad. Sci. U.S.A.* **89**, 3285 (1992).
  16. EcoRI DNAs (10  $\mu$ g of each) were digested with Eco RI. The fragments were separated by gel electrophoresis and blotted on GeneScreenPlus membranes (NEN) as recommended by the manufacturer. The mouse *Pou3f4* genomic segment was amplified from 500 ng of mouse genomic DNA, 250 ng of the primers 977 [nucleotides 119 to 140 of the *POU3F4* open reading frame (ORF) (19); GTGACTACTTGCAGGGAGTTCC] and 978 (nucleotides 521 to 540 of the ORF; GCAGTGGTCCGAGC-CAGACT; Isogen Biosciences), 10 mM tris-HCl (pH 8.0), 50 mM KCl, 3 mM MgCl<sub>2</sub>, and 0.01% gelatin. After initial denaturation for 5 min at 94°C, amplification was done in 30 cycles of 1 min at 94°C, 1 min at 64°C, and 1 min at 72°C, with a final elongation step for 6 min at 72°C. The PCR product was purified from low melting temperature (LMT) agarose and radiolabeled with the use of random hexamer priming. The blot in Fig. 1A was hybridized in 0.5 M NaH<sub>2</sub>PO<sub>4</sub> (pH 6.8), 7% (w/v) SDS, 1 mM EDTA, and 50  $\mu$ g/ml of sonicated, denatured herring sperm DNA at 55°C for 18 hours. Washing was done in 40 mM NaH<sub>2</sub>PO<sub>4</sub> and 1% (w/v) SDS at 60°C for 1 hour. The mouse *Alas2* cDNA probe pMS20 [D. S. Schoenhaut and P. J. Curtis, *Gene* **48**, 55 (1986)] was hybridized to the blot shown in Fig. 1A, as described for the mouse *Pou3f4* probe. The gene encoding human ALAS2 is located in Xp11.2 [P. D. Cotter, H. F. Willard, J. L. Gorski, D. F. Bishop, *Genomics* **13**, 211 (1992)].
  17. We used the mouse *Pou3f4* primers 977 and 978 (16) to amplify a 420-bp segment of the human *POU3F4* gene using 10 ng of cosmid IC3. The PCR product was purified in an LMT agarose gel and labeled as described (16). Phage recombinants (10<sup>9</sup>) of a fetal brain cDNA library (Stratagene) were screened with this DNA fragment, as described [F. P. M. Cremers, D. J. R. van de Pol, L. P. M. van Kerkhoff, B. Wieringa, H.-H. Ropers, *Nature* **347**, 674 (1990)]. Six cDNA clones were isolated, four of which were analyzed further. The ORF of the human *POU3F4* gene was sequenced on both strands with the use of mouse and human *POU3F4* oligonucleotides that amplified DNA from cosmid IC3 and DNA from the four cDNA clones. Sequences from the 5' and 3' untranslated regions were obtained from the cDNA clones. Sequence analysis was performed with the dye terminator sequencing kit on an Applied Biosystems automated sequencer. The human *POU3F4* cDNA sequence has been deposited in the European Molecular Biology Laboratory database with accession number X82324.
  18. Y. Hara, A. C. Rovescalli, Y. Kim, M. Nirenberg, *Proc. Natl. Acad. Sci. U.S.A.* **89**, 3280 (1992).
  19. J. M. Mathis *et al.*, *EMBO J.* **11**, 2551 (1992).
  20. PCR-SSC analysis [M. Orita, Y. Suzuki, T. Sekiya, K. Hayashi, *Genomics* **5**, 874 (1989)] was performed with five partially overlapping PCR products that span the ORF of *POU3F4*. We added 250 ng of each primer from the five sets of primers (Ia (ACTAGTAGGGGATCCTCACCG) and Ib (CCGTCGCTCAGACTGGTCAAC); IIa (GTGACTACTTGCAGGGAGTTCC) and IIb (CCAGCATACCGTCAACCGTG); IIIa (ACGTGTACTCGCAGCCTGGC) and IIIb (CGGICTCGCGTGAAGCCCAAC); IVa (GATGAGTTGGAACA-GTTTCGCCAA) and IVb (TGACACTCACTCGATG-GAGG); and Va (CATTGACAAGATGCTGCAAC) and Vb (GCCTCCTCGCTTCTCCCA)] to buffers containing either 10 mM tris-HCl (pH 8.0), 50 mM KCl, 3 mM MgCl<sub>2</sub>, and 0.01% gelatin (primer set I), 10 mM tris-HCl (pH 8.0), 50 mM KCl, 2 mM MgCl<sub>2</sub>, and 1 mM dithiothreitol (primer sets II, IV, and V), or 30 mM tricine-HCl (pH 8.4), 2 mM MgCl<sub>2</sub>, 0.01% gelatin, and 5 mM  $\beta$ -mercaptoethanol (primer set III), supplemented with 500 ng of genomic DNA, 4 mM deoxyadenosine triphosphate, deoxyguanosine triphosphate, and deoxythymidine triphosphate (dATP), 1 mM deoxycytidine triphosphate (dCTP), 1  $\mu$ Ci of [ $\alpha$ -<sup>32</sup>P]dGTP, and 1 unit of Taq DNA polymerase (Boehringer). After initial denaturation for 5 min at 94°C, amplification was done in 30 cycles of 1 min at 94°C, 1 min at 64°C (primer sets I through IV), or 1 min at 58°C (primer set V) and 1 min at 72°C

- with a final elongation step for 6 min at 72°C. The PCR products were separated on a 6% polyacrylamide gel, with or without 10% (w/v) glycerol, for 4 hours at 35 W at 4°C. After vacuum drying, the gels were exposed to Xomat films (Kodak) for 18 hours at room temperature. The sequence of PCR products was established for both strands as described (17). Primers Ia, IIb, and IIIb were deduced from mouse *Pou3f4* sequences. The nucleotides that do not match the human *POU3F4* sequence are underlined above. The sequence shown in Fig. 3B was established with the use of <sup>32</sup>P end-labeled primer Va with the cycle sequencing kit (Boehringer).
21. Mutations are indicated with the single-letter amino acid abbreviations; thus, Leu<sup>317</sup>  $\rightarrow$  Trp is indicated by L317W. Abbreviations for the amino acid residues are A, Ala; C, Cys; D, Asp; E, Glu; F, Phe; G, Gly; H, His; I, Ile; K, Lys; L, Leu; M, Met; N, Asn; P, Pro; Q, Gln; R, Arg; S, Ser; T, Thr; V, Val; W, Trp; and Y, Tyr.
  22. J. D. Klemm *et al.*, *Cell* **77**, 21 (1994).
  23. C. A. Pabo and R. T. Sauer, *Annu. Rev. Biochem.* **61**, 1053 (1992).
  24. K. Okamoto *et al.*, *J. Biol. Chem.* **268**, 7449 (1993).
  25. C. R. Kissinger *et al.*, *Cell* **63**, 579 (1990).
  26. This was determined by the two-sided Fisher's exact test;  $P < 0.001$ .
  27. A. Lalwani *et al.*, *Am. J. Hum. Genet.* **53**, 1027 (1993); M. Bitner-Glindzicz *et al.*, *J. Med. Genet.* **31**, 916 (1994).
  28. A. F. Ryan, E. B. Crenshaw III, D. M. Simmons, *Ann.*

- N.Y. Acad. Sci.* **630**, 129 (1991).
29. P. Thorpe *et al.*, *S.A. Med. J.* **48**, 587 (1974).
  30. Personal communications of K. Shaver-Amos (patients 3055 and 3056), O. Michel (patient 3105), I. van Langen and R. Hennekam (patient 5823), H. G. Brunner (patients 2266 and 2418), M. Stul (patient 2964), and J. Gouldsmith (patient 3036).
  31. The authors are indebted to P. Beighton, J. Gouldsmith, R. Hennekam, I. van Langen, O. Michel, W. E. Nance, W. P. Reardon, N. Stul, K. Shaver-Amos, and P. Thorpe for providing blood and information of patients with X-linked deafness. We are especially grateful to H. G. Brunner for his support of this project. We thank I. H. J. M. Scholten, S. D. van der Velde-Visser, and E. Boender-van Rossum for excellent technical assistance and J. Hendriks for statistical analysis. We thank Y. Ishikawa-Brush for YAC screening and M. Ross, G. Zehetner, and H. Lehrach for access to the Imperial Cancer Research Fund cosmid library filters and the Reference Library Database, London. The research of F.P.M.C. has been made possible by a fellowship of the Royal Netherlands Academy of Arts and Sciences. M.B.-G. is a Medical Research Council Clinical Training Fellow. M.E.P. is funded by Mothercare. This work was supported by the Netherlands Organization for Scientific Research (NWO), by the European Community, and by the Imperial Cancer Research Fund.

22 September 1994; accepted 28 December 1994

## Requirement of MADS Domain Transcription Factor D-MEF2 for Muscle Formation in *Drosophila*

Brenda Lilly, Bin Zhao, Gogineni Ranganayakulu, Bruce M. Paterson, Robert A. Schulz, Eric N. Olson\*

Members of the myocyte enhancer binding factor-2 (MEF2) family of MADS (MCM1, agamous, deficiens, and serum response factor) box transcription factors are expressed in the skeletal, cardiac, and smooth muscle lineages of vertebrate and *Drosophila* embryos. These factors bind an adenine-thymidine-rich DNA sequence associated with muscle-specific genes. The function of MEF2 was determined by generating a loss-of-function of the single *mef2* gene in *Drosophila* (*D-mef2*). In loss-of-function embryos, somatic, cardiac, and visceral muscle cells did not differentiate, but myoblasts were normally specified and positioned. These results demonstrate that different muscle cell types share a common myogenic differentiation program controlled by MEF2.

The three major muscle cell types (skeletal, cardiac, and smooth) express many of the same muscle-specific genes, which suggests that they may use a common myogenic regulatory program that directs muscle gene transcription. However, each muscle cell type is unique with respect to the muscle proteins expressed, contractile properties, ability to divide, and morphology. Thus, if a common myogenic program exists, it must be modified by additional regulatory factors to generate muscle cell diversity.

B. Lilly, B. Zhao, G. Ranganayakulu, R. A. Schulz, E. N. Olson, Department of Biochemistry and Molecular Biology, The University of Texas M. D. Anderson Cancer Center, Houston, TX 77030, USA.  
B. M. Paterson, Laboratory of Biochemistry, National Cancer Institute, National Institutes of Health, Bethesda, MD 20892, USA.

\*To whom correspondence should be addressed.

In vertebrates, skeletal muscle formation is controlled by a family of myogenic basic helix-loop-helix (bHLH) proteins, which includes MyoD, myogenin, myf5, and MRF4 [reviewed in (1)]. When expressed ectopically in nonmuscle cell types, these factors can activate skeletal muscle gene expression. The myogenic bHLH factors are exclusively expressed in skeletal muscle. Therefore, other regulators must control muscle gene expression in cardiac and smooth muscle. MEF2, which recognizes an A-T-rich DNA sequence associated with skeletal, cardiac, and smooth muscle genes, may be such a factor (2). Four *mef2* genes, designated *mef2a*, *-b*, *-c*, and *-d*, have been cloned from several vertebrate species (3, 4). MEF2 factors, also known as related to serum response factors (RSRFs) (4), belong to the MADS family of transcription factors

and share extensive homology in the MADS domain, which mediates dimerization and DNA binding.

Recent studies have implicated MEF2 factors in the regulation of myogenic bHLH genes. MEF2-binding sites in the promoters of the mouse *myogenin* (5) and *Xenopus MyoD* (6) genes are important for transcription of these genes in muscle cells. Expression of exogenous MEF2 factors in fibroblasts can induce the expression of myogenic bHLH genes (7). Conversely, MEF2 DNA-binding activity can be induced in nonmuscle cells by myogenic bHLH factors (8). Thus, myogenic bHLH proteins and MEF2 factors function within a regulatory network that involves positive feedback loops in which the two families of factors cross-regulate one another's expression.

The functions of the MEF2 family may be difficult to define in vertebrate systems because there are multiple *mef2* genes with overlapping expression patterns (9). Therefore, we have sought to define the functions of MEF2 in *Drosophila*, which contains a single *mef2* gene, *D-mef2*, that encodes a protein with extensive homology to the MADS domains of the mammalian MEF2 proteins (10, 11). During embryogenesis, *D-mef2* expression is initiated at gastrulation within mesodermal precursor cells in the ventral furrow. Shortly thereafter, *D-mef2* expression becomes restricted to the somatic, cardiac, and visceral muscle lineages. The conserved structure and DNA-binding activity of the D-MEF2 protein and the restricted expression of the *D-mef2* gene to myogenic lineages of the *Drosophila* em-

bryo suggest that *D-mef2* and the mammalian *mef2* genes perform similar functions in muscle development.

In vertebrates, MEF2 transcripts are present in all cell types, whereas MEF2 DNA-binding activity is largely restricted to muscle cells (2–4). To determine the cell types in which D-MEF2 might be functional, we stained *Drosophila* embryos with an antibody to D-MEF2. The D-MEF2 protein was first detected in mesodermal cells within the ventral furrow at the cellular blastoderm stage (Fig. 1A). During germ band extension, D-MEF2 became expressed throughout the mesoderm and was absent from the overlying ectoderm and the endoderm primordia (Fig. 1B). At stage 11, the mesoderm separates to form the somatopleura and splanchnopleura, which give rise to the somatic and visceral musculature, respectively (12). D-MEF2 was expressed in all of these muscle cell precursors at this stage, including the precardiac cells, which are derived from the dorsal-most two rows of mesodermal cells (Fig. 1, C and D). Subsequently, as the somatic and visceral muscle differentiated, D-MEF2 was expressed in all somatic and pharyngeal muscle cell nuclei, as well as in visceral muscle of the fore-, mid-, and hindgut. D-MEF2 expression was also observed in the two rows of cardioblasts within the dorsal vessel (Fig. 1, E to G). Within the somatic muscle, D-MEF2 expression exhibited a segmentally repeating pattern that demarcated the positions of the ventral, pleural, and dorsal muscle cells (Fig. 1, F and G). As the mesoderm gave rise to different derivatives, D-MEF2 expression became restricted to muscle cells, with no expression in other mesodermal structures, such as the fat body. We detected no somatic, visceral, or cardiac muscle cells that did not express D-MEF2 protein. Thus, the expression of D-MEF2 protein parallels that of *D-mef2* mRNA and marks all of the muscle cell precursors and their descendants in the embryo.

To initiate a genetic analysis of *D-mef2*, we isolated and characterized the *D-mef2* gene, which spans ~13.5 kb and contains eight exons (Fig. 2A). The ATG codon for translation initiation is located in exon 2, which is preceded by a 6-kb intron. Intron 2 splits the MADS domain after codon 18, and intron 3 defines the end of the MEF2 domain (codon 86), which is also conserved among members of the MEF2 family. The positions of these two introns are conserved to the exact codons in the four mouse *mef2* genes (13).

Because we planned to screen for null alleles of *D-mef2*, which could in principle arise from mutations in the coding or regulatory regions of the gene, we tested wheth-

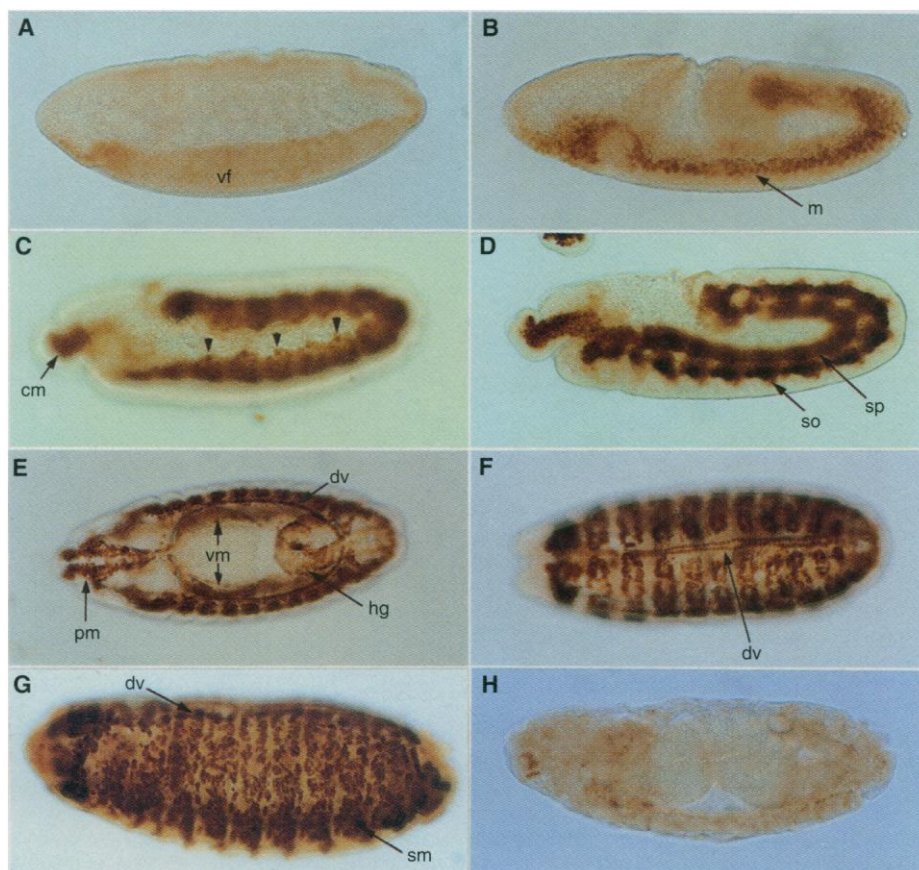


**Fig. 1.** Expression of D-MEF2 during embryogenesis. D-MEF2 protein was detected by immunostaining (34) of *Drosophila* embryos with an antibody to D-MEF2 (anti-D-MEF2) (35). **(A)** Lateral view of cellular blastoderm stage 6 embryo showing D-MEF2 expression in ventral furrow (vf). **(B)** Lateral view of germ band-extended stage 8 embryo showing D-MEF2 expression throughout the mesoderm (m). **(C)** Lateral view of late germ band-extended stage 10 embryo showing D-MEF2 expression throughout the mesoderm, in heart precursors (indicated by arrowheads), and cephalic mesoderm (cm). **(D)** Lateral view of early germ band-retracting stage 12 embryo showing D-MEF2 expression in the somatopleura (so) and splanchnopleura (sp). **(E)** Dorsal view of stage 14 embryo showing D-MEF2 expression in hindgut (hg), visceral mesoderm (vm), and pharyngeal muscle (pm). At this stage, precursors of the dorsal vessel (dv) can be seen lying along both sides of the embryo. Somatic muscle cells are arranged laterally within each segment. **(F)** Dorsal view of stage 16 embryo at the time of dorsal closure. D-MEF2 expression can be seen throughout the somatic muscles and in the two rows of cardioblasts composing the dorsal vessel. **(G)** Lateral view of stage 16 embryo flattened to show D-MEF2 expression in nuclei of somatic musculature (sm). **(H)** Lateral view of *Df(2R)P544* homozygous embryo (stage 15). No specific staining above background is detected.

er the region immediately upstream of *D-mef2* contained sequences sufficient to direct *D-mef2* transcription in early mesoderm and in myogenic lineages. A 4-kb Eco RI fragment extending upstream from exon 1 was inserted in front of a *lacZ* reporter gene, and the transgene was introduced into the *Drosophila* germ line by P-element transformation (14). This *D-mef2* promoter fragment directed the expression of *lacZ* at a low level in the ventral mesoderm beginning at the late cellular blastoderm stage. Expression was then observed at high levels in somatic and visceral muscle cell precursors during germ band extension (Fig. 2, C and D) and throughout the differentiated somatic and visceral musculature by stage 13–14 (Fig. 2, F and G). We did not detect *D-mef2-lacZ* expression in the dorsal vessel. Thus, the regulatory elements required for visceral and somatic muscle expression are contained in the proximal 5' flanking region of the gene, whereas elements for cardiac muscle expression are apparently located elsewhere.

On the basis of the mesoderm- and muscle-specific pattern of expression, we anticipated that loss-of-function mutations in *D-mef2* would result in embryonic lethality as a result of severe muscle defects. We therefore conducted a P-element insertional mutagenesis screen to identify potentially lethal *D-mef2* mutant alleles. Before initiating the screen, the cytological location of *D-mef2* was mapped to the 46C interval of the right arm of chromosome 2 (10). The proximal breakpoints of two overlapping deficiencies within the 46C region, *Df(2R)X1* (15) and *Df(2R)eve<sup>1.27</sup>* (16), were mapped relative to the location of *D-mef2* (17). The *Df(2R)X1* deficiency breaks within the first intron of *D-mef2* and extends distally to the 46F interval upstream of the gene (Fig. 2A) (15). This mutation eliminated all detectable *D-mef2* expression (18). The *Df(2R)eve<sup>1.27</sup>* deficiency extends from ~16 kb 5' of *D-mef2*, leaving *D-mef2* expression unaffected.

For the P-element mutagenesis screen, we used a homozygous viable P-element insertion line P[*lArB*]2487 (19) that carries a single P element integrated ~25 kb 5' of the *D-mef2* transcription initiation site (Fig. 2A). Because P elements transpose at a higher frequency to nearby positions (20), we mobilized P2487 and screened for insertions that were lethal in trans to *Df(2R)X1* (21). One lethal line, designated P544, was found to harbor a deletion that extended from the original P2487 insertion site to 320-base pairs (bp) upstream of *D-mef2* (Fig. 2A).

Complementation tests showed that the P544 mutation was embryonic lethal when homozygous or when hemizygous in trans to *Df(2R)X1*, whereas it was viable when hem-

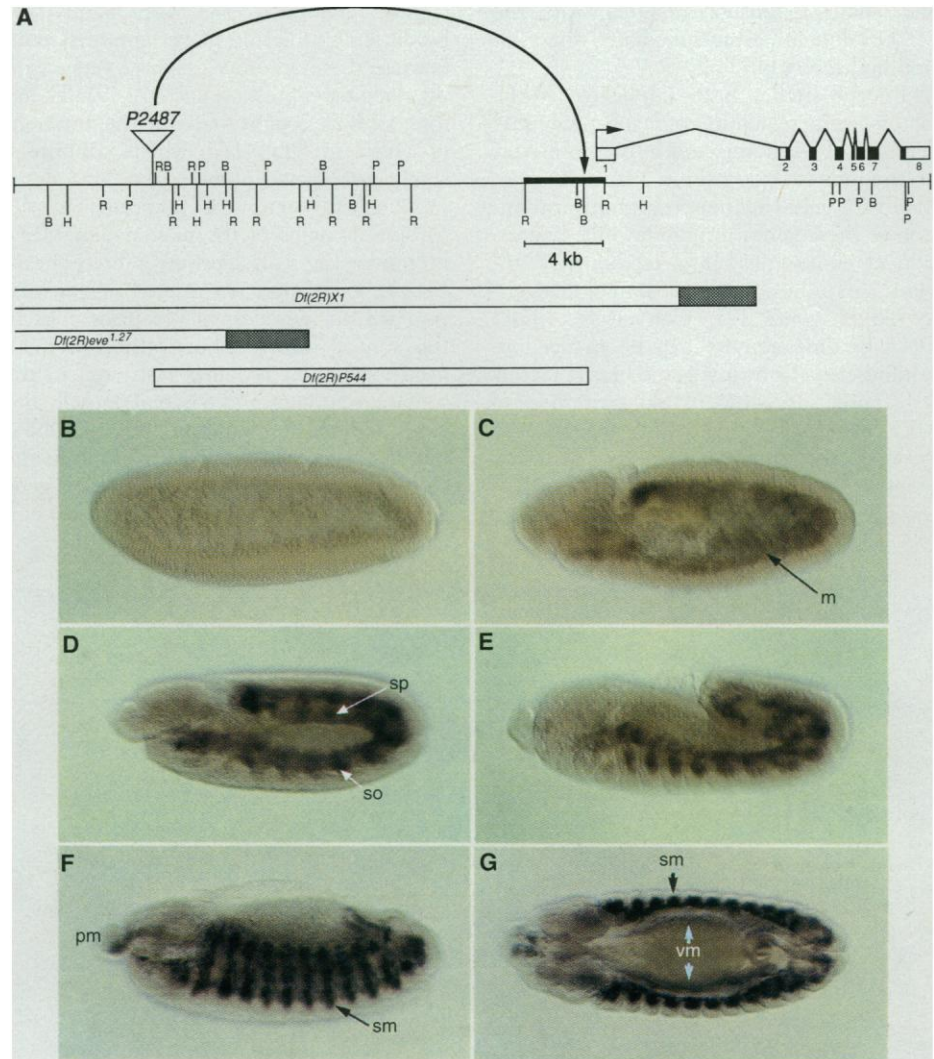


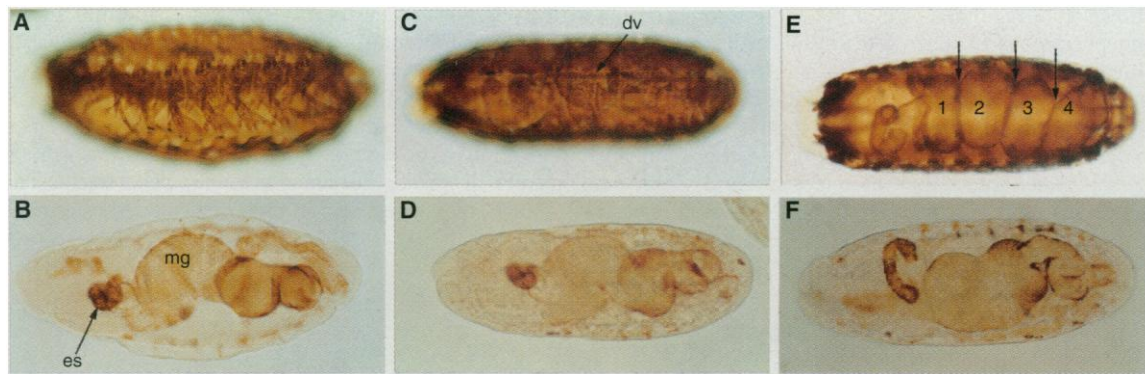
**Fig. 2.** Structure and expression of the *D-mef2* gene. **(A)** Genomic clones spanning the *D-mef2* gene were isolated, and the positions of exons were determined (17). All introns except intron 1 were sequenced in their entirety. Positions of restriction sites are shown: B, Bam HI; H, Hind III; P, Pst I; and R, Eco RI. Coding and noncoding regions are indicated in black and white, respectively (36). The transcription initiation site, designated by a horizontal arrow above exon 1, was determined by primer extension and RNase protection (18). The position of P2487 insertion is indicated at the top, and the position to which the P element was mobilized is indicated by the arrow to the thick black line, which represents the promoter fragment used to create the *D-mef2-lacZ* reporter. The deleted regions of the *Df(2R)X1*, *Df(2R)eve<sup>1.27</sup>*, and *Df(2R)P544* alleles are shown at the bottom. Filled regions of the boxes denote the regions of the proximal breakpoints. The distal breakpoints of the *Df(2R)X1* and *Df(2R)eve<sup>1.27</sup>* deletions extend beyond the genomic region shown (15). **(B to G)** Expression of a *D-mef2-lacZ* reporter gene during embryogenesis (14). **(B)** Lateral view of an early gastrula stage 5 embryo. **(C)** Lateral view of germ band-extended stage 9 embryo showing  $\beta$ -galactosidase expression throughout the presumptive mesoderm (m). **(D)** Lateral view of late germ band-extended stage 11 embryo. Somatopleura, so; splanchnopleura, sp. **(E)** Lateral view of germ band-retracting stage 12 embryo. **(F)** Lateral view of stage 13 embryo showing expression in pharyngeal muscle (pm) and somatic muscle (sm). **(G)** Dorsal view of stage 14 embryo showing  $\beta$ -galactosidase expression in somatic muscle (sm) and visceral muscle (vm).

izygous in trans to *Df(2R)eve<sup>1.27</sup>*. Because *D-mef2* is expressed in embryos homozygous for the *Df(2R)eve<sup>1.27</sup>* deficiency (18), we conclude that the ~16-kb region of non-overlap between the *Df(2R)eve<sup>1.27</sup>* and *Df(2R)P544* deficiencies contains the regulatory elements required for *D-mef2* expression. Within the region that was deleted by the P544 mutation, there are no known lethal complementation groups (15), which

suggests that this deletion did not eliminate other essential genes. Moreover, embryos transheterozygous for *Df(2R)P544* and a recently identified, severe, ethylmethane sulfonate (EMS)-induced point mutant of *D-mef2* show a muscle phenotype comparable with that seen in *Df(2R)P544* homozygous embryos (22).

The homozygous P544 mutation resulted in a loss of D-MEF2 protein (Fig. 1H) and

**Fig. 3.** Expression of MHC in wild-type and *D-mef2* mutant embryos. Myosin expression was detected by immunostaining of stage 16 embryos (34). (A and B) Lateral view. (C and D) Dorsal view. (E and F) Ventral view. The three constrictions that subdivide the midgut into four chambers (labeled 1 to 4) are shown with arrows in (E). Esophagus (es); dorsal vessel, dv; midgut, mg. (A), (C), and (E) are wild-type embryos. (B), (D), and (F) are *P544* homozygous mutant embryos.



mRNA (18) expression in embryos. The loss of expression of the *D-mef2* gene in *P544* mutant embryos suggests that important regulatory elements upstream of the proximal breakpoint of *Df(2R)P544* at  $-320$  bp were deleted by the P-element mobilization. Because expression of *D-mef2* in the dorsal vessel was lost in *P544* embryos, and the 3.4-kb 5' flanking region of *D-mef2* did not direct expression in the dorsal vessel, we conclude that this expression depends on sequences upstream of  $-3.4$  kb.

To determine the consequences of the *P544* mutation on muscle gene expression, we analyzed embryos homozygous for *Df(2R)P544* and transheterozygous for *Df(2R)X1* and *Df(2R)P544*. Embryos of the two mutant genotypes showed comparable phenotypes. The *P544* mutant embryos were readily identifiable by the apparent absence of any somatic muscle and a severely bloated midgut, which appeared to result from a lack of differentiated visceral muscle cells. As a marker for muscle formation, we stained embryos for myosin heavy chain (MHC) expression, which serves as a marker for the somatic muscle of the body wall, cardiac muscle of the dorsal vessel, and visceral muscle of the gut (23). There was virtually no MHC staining of the somatic muscles in mutant embryos (Fig. 3), nor was there any evidence of myoblast fusion, on the basis of staining with toluidine blue (18), which allows visualization of multinucleated myotubes (12). There was also no detectable expression of MHC in the cardiac cells of the dorsal vessel or in the visceral muscle-derived alary muscles that suspend the mature heart tube from the epidermis (Fig. 3). MHC expression was detected at a very low level in a few striated visceral muscle cells that line the gut of mutant embryos. The only region of the mutant embryos in which MHC was expressed at significant levels was the esophagus, just anterior to the midgut (Fig. 3). Other markers of muscle differentiation also were not expressed in the three myogenic lineages of mutant embryos, but they were expressed in the esophagus (18).

The loss of MHC expression in *D-mef2* mutant embryos could be the result of an inability of myoblasts to differentiate or the result of a block in commitment of mesodermal progenitors to myogenic lineages. To distinguish between these possibilities, we examined the expression of several genes that mark uncommitted mesoderm and committed mesodermal progenitors of the three myogenic lineages. The *Drosophila* fibroblast growth factor receptor (DFR1) marks all cells of the mesoderm destined to form muscle, as well as other mesodermal derivatives, and shows an expression pattern in the early mesoderm similar to that of *D-mef2* (24). DFR1 expression was normal in *P544* mutant embryos (Fig. 4, A and B) and was refined to a subset of somatic muscle cell precursors normally.

The homeobox gene *tinman* is coexpressed with *D-mef2* in the ventral mesoderm and subsequently becomes restricted to the dorsal vessel (25, 26). The expression of *tinman* in the early mesoderm and in the dorsal vessel was identical in wild-type and *P544* embryos (Fig. 4, C and D). The *P544* mutation also had no effect on expression of *bagpipe* (Fig. 4, E and F), a homeobox gene expressed after *tinman* in the dorsal vessel as well as in segmental precursors of the visceral muscle of the gut (26).

The extracellular matrix molecule fasciclin-III (FAS-III) is expressed in visceral mesoderm that gives rise to the visceral muscles of the gut, which are arranged as two layers of mononucleated muscle cells that provide the force for peristaltic movements of digestion (27). In *D-mef2* mutant embryos, FAS-III expression was normal (Fig. 4, G and H), and FAS-III-expressing cells migrated normally around the underlying endoderm to form a completed midgut tube. However, the gut of the mutant embryos did not elongate and had a bloated appearance. The midgut normally contains three well-defined constrictions, which were still detectable in mutant embryos.

Somatic muscle in *Drosophila* is composed of multinucleate muscle fibers, organized in a repeating pattern in each he-

misegment (12). In mutant embryos, the somatic muscle cells remained unfused and did not express MHC (Fig. 3). The myogenic bHLH gene *nautilus/D-myf* and the homeobox genes *apterous* and *S59* are expressed in distinct subsets of somatic muscle cell precursors in each hemisegment beginning at stage 11 (28–30). The expression patterns of *nautilus*, *apterous*, and *S59* in muscle cell precursors were unaffected in *D-mef2* mutant embryos (Fig. 4, I to M). At later stages, *S59* expression could be seen in the syncytia of distinct groups of myotubes in normal embryos (Fig. 4M), whereas in mutant embryos *S59*-expressing cells remained in unorganized clusters in their original segmental pattern (Fig. 4N).

Together, these results demonstrate that *D-mef2* is essential for the differentiation of muscle cells from all three myogenic lineages in the *Drosophila* embryo: somatic, cardiac, and visceral. In the absence of *D-mef2* expression, muscle cell precursors are correctly specified and positioned, but they are unable to express muscle structural genes. The phenotype of *D-mef2* mutant embryos suggests that *D-mef2* acts at a relatively late stage within different myogenic lineages to control differentiation. Given that MEF2-binding sites are found in the control regions of numerous muscle-specific genes in *Drosophila* (18) and mammals (2, 5), we propose that MEF2 factors are involved in the direct activation of muscle-specific genes during differentiation of these different muscle cell types.

Our results begin to define the hierarchy of regulatory genes leading from uncommitted mesoderm to the formation of differentiated muscle cells in the *Drosophila* embryo. The genes *tinman* and *D-mef2* are expressed concomitantly in the ventral mesoderm during embryogenesis (10, 11). Previously, we showed that *D-mef2* was expressed in *tinman* mutant embryos (10), and here we show that *tinman* is expressed in *D-mef2* mutant embryos. Thus, *tinman* and *D-mef2* are expressed independently and perhaps respond to a common upstream regulator. The gene *bagpipe*, which was previously

shown to be regulated by *tinman* (26), is also independent of *D-mef2*. Within the cardiac lineage, the function of *D-mef2* contrasts with that of *tinman*. In *tinman* mutant embryos, the dorsal vessel fails to form (25, 26), whereas in *D-mef2* mutant embryos the dorsal vessel forms, but muscle structural genes are not expressed. A similar case is

found in the visceral muscles surrounding the midgut. In *tinman* mutants, the visceral mesoderm does not form and the underlying endoderm fails to migrate to form a fused tube (25, 26). In *D-mef2* mutants, midgut migration is normal; however, the gut is morphologically distorted, presumably because of a lack of expression of muscle

structural proteins. It is intriguing that a subset of visceral muscle cells within the esophagus retained the ability to differentiate in the absence of D-MEF2 protein, which suggests the existence of an alternate pathway for muscle gene activation in these cells. In the somatic muscle lineage, *nautilus* and the homeobox genes *apterous* and *S59* are also expressed independently of *D-mef2*. Thus, the specification of somatic muscle precursor cells in each hemisegment is not controlled by *D-mef2*, whereas the process of myoblast fusion is dependent on the expression of *D-mef2*. The independence of *nautilus* expression of D-MEF2 appears to differ from certain of the vertebrate myogenic bHLH genes, which have been shown to be regulated by MEF2 (5, 6). Whether *nautilus* is regulated by D-MEF2 later in development remains to be determined.

Thus far, *D-mef2* is the only example of a gene that controls differentiation in multiple muscle cell types. The virtual absence of muscle gene expression in *D-mef2* mutant embryos suggests that D-MEF2 establishes a basic myogenic program that directs the expression of muscle-specific genes. However, because somatic, cardiac, and visceral muscle cells are distinct, this MEF2-dependent regulatory program must be modified through the action of other factors to generate muscle cell diversity.

#### REFERENCES AND NOTES

1. C. P. Emerson Jr., *Curr. Opin. Cell Biol.* **2**, 21065 (1990); M. Buckingham, *Trends Genet.* **8**, 144 (1992); H. Weintraub, *Cell* **75**, 1241 (1993); W. E. Wright, *Curr. Opin. Genet. Dev.* **2**, 243 (1993); E. N. Olson and W. H. Klein, *Genes Dev.* **8**, 1 (1994).
2. L. A. Gossett, D. J. Kelvin, E. A. Sternberg, E. N. Olson, *Mol. Cell. Biol.* **9**, 5022 (1989).
3. Y.-T. Yu *et al.*, *Genes Dev.* **6**, 1783 (1992); D. Leifer *et al.*, *Proc. Natl. Acad. Sci. U.S.A.* **90**, 1546 (1993); J. C. McDermott *et al.*, *Mol. Cell. Biol.* **13**, 2564 (1993); R. E. Breitbart *et al.*, *Development* **118**, 1095 (1993); J. F. Martin, J. J. Schwarz, E. N. Olson, *Proc. Natl. Acad. Sci. U.S.A.* **90**, 5282 (1993); J. F. Martin *et al.*, *Mol. Cell. Biol.* **14**, 1647 (1994).
4. R. Pollock and R. Treisman, *Genes Dev.* **5**, 2327 (1991).
5. D. G. Edmondson, T.-C. Cheng, P. Cserjesi, T. Chakraborty, E. N. Olson, *Mol. Cell. Biol.* **12**, 3665 (1992); T.-C. Cheng, M. Wallace, J. P. Merlie, E. N. Olson, *Science* **261**, 215 (1993); S. P. Yee and W. J. Rigby, *Genes Dev.* **7**, 1277 (1993).
6. D. Leibham *et al.*, *Mol. Cell. Biol.* **14**, 686 (1994).
7. S. Kaushal, J. W. Schneider, B. Nadal-Ginard, V. Mahdavi, *Science* **266**, 1236 (1994); J. Martin, B. Black, A. Firulli, E. N. Olson, unpublished data.
8. P. Cserjesi and E. N. Olson, *Mol. Cell. Biol.* **11**, 4854 (1991); A. B. Lassar *et al.*, *Cell* **66**, 305 (1991).
9. A. E. Chambers, S. Kotecha, N. Towers, T. J. Mohun, *EMBO J.* **11**, 4981 (1992); D. Edmondson, G. Lyons, J. F. Martin, E. N. Olson, *Development* **120**, 1251 (1994).
10. B. Lilly, S. Galewsky, A. B. Firulli, R. A. Schulz, E. N. Olson, *Proc. Natl. Acad. Sci. U.S.A.* **91**, 5662 (1994).
11. H. Nguyen *et al.*, *ibid.*, p. 7520.
12. M. Bate, in *The Development of Drosophila melanogaster*, M. Bate and A. M. Arias, Eds. (Cold Spring Harbor Laboratory Press, Cold Spring Harbor, NY, 1993), vol. 3, pp. 1013-1090.
13. J. Martin, B. Lilly, B. Black, E. N. Olson, unpublished data.
14. A 4.0-kb Eco RI DNA fragment encompassing 3.4 kb

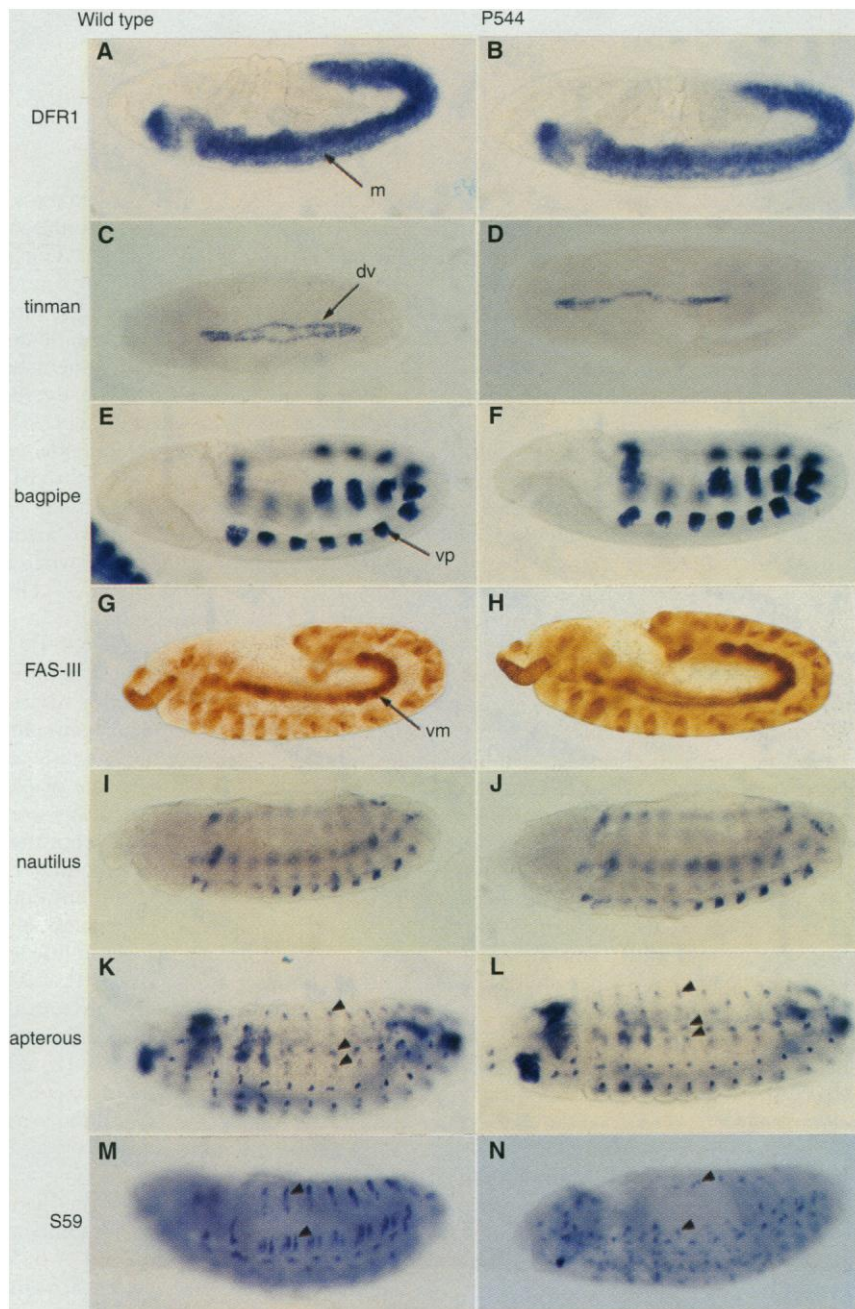


**Fig. 4.** Expression of mesodermal markers in wild-type and *D-mef2* mutant embryos. Expression of mesodermal markers was detected by immunostaining (34) or in situ hybridization (38) to wild-type (A, C, E, G, I, and K) and *P544* mutant (B, D, F, H, J, and L) embryos. (A and B) DFR1 mRNA in stage 8 embryos (24); (C and D) *tinman* mRNA in stage 16 embryos (25); (E and F) *bagpipe* mRNA in stage 10 embryos (26); (G and H) FAS-III protein in stage 11 embryos (27); (I and J) *nautilus* mRNA in stage 14 embryos (28); (K and L) *apterous* mRNA in stage 14 embryos (29). (M and N) S59 mRNA in stage 14 embryos (34). Dorsal vessel, dv; mesoderm, m; visceral mesoderm, vm; visceral muscle precursors, vp. The arrowheads in (K) through (N) point to subsets of somatic muscle cell precursors that express the genes *apterous* and S59, respectively. In (M), the expression of S59 protein can be seen in multinucleate myotubes, whereas in (N), only mononucleate cells are seen.

- of the *D-mef2* 5' flanking sequence and 0.6 kb of exon 1 was cloned into the P-element transformation vector CaSpeR AUG- $\beta$ -gal (31) to generate a *D-mef2-lacZ* transgene. This sequence was stably introduced into the *Drosophila* genome by P element-mediated germline transformation [G. M. Rubin and A. C. Spradling, *Science* **218**, 348 (1982)]. The *yw<sup>57c23</sup>* strain was used for embryo injections, and flies transformed with *D-mef2-lacZ-CaSpeR* were identified by *w<sup>+</sup>* selection. Similar expression patterns were observed in six independent lines.
15. M. A. O'Brien, M. S. Roberts, P. H. Taghert, *Genetics* **137**, 121 (1994).
  16. Strains *Df(2R)veve<sup>1,27</sup>/CyO* and *b Adh cn/CyO; ry<sup>506</sup>* were obtained from the Bloomington stock center; *Df(2R)X1/CyO* was a gift from M. O'Brien and P. Taghert (Washington University Medical Center, St. Louis, MO); *Sp/CyO; ry506Sb P[ry+ $\Delta$ 2-3](99B)/TM6,Ubx* was obtained from W. Mattox (M. D. Anderson Cancer Center, Houston, TX); and *P[lacZ,ry+J2487* was obtained from R. Davis (Baylor College of Medicine, Houston, TX).
  17. Isolation of genomic clones and the restriction mapping and Southern (DNA) blot analysis to map the *D-mef2* gene, the deficiency breakpoints, and P-element insertions were performed as described (32). Primer extension and ribonuclease (RNase) protections to map the transcription site were done according to the manufacturer's protocol (Ambion), as described (32).
  18. B. Lilly, thesis, The University of Texas, Houston (1995).
  19. R. Davis, personal communication.
  20. J. Tower, G. H. Karpem, N. Craig, A. C. Spradling, *Genetics* **133**, 347 (1993); P. Zhang and A. C. Spradling, *ibid.*, p. 361.
  21. The P-element mobilization strategy was based on those described (20). Homozygous viable P element, *P[lacZ,ry+J2487*, residing near the *D-mef2* locus was mobilized by introducing the  $\Delta$ 2-3 transposase into the stock. Female flies from this cross, genotype *P[lacZ,ry+]/CyO;ry<sup>506</sup>Sb P[ry+ $\Delta$ 2-3](99B)*, were collected, and the P element was stabilized by crossing out the  $\Delta$ 2-3 transposase by mating to *b Adh cn/CyO; ry<sup>506</sup>*. Single males with a putative *D-mef2* insertion from the mobilized *P[lacZ,ry+J2487\*/CyO;ry<sup>506</sup>* were screened for lethal mutations over the *Df(2R)X1/CyO* that spans the *D-mef2* locus. Screening of 1000 lines with a potentially transposase-mobilized 2487 P element yielded 15 lines that were lethal in trans to the deficiency. We determined which, if any, of the lethal lines contained a P-element insertion that disrupted *D-mef2* expression by balancing individual lethal lines over *CyO* and screening genomic DNA from the lines by PCR, using a pool of primers from *D-mef2* and the terminal repeat at each end of the P element (33). One lethal line, designated P544, was identified in which a PCR product was generated. The *D-mef2* primer that, in combination with the P-element primer, produced the PCR product was identified by performing the reactions with individual primers. Further mapping and sequencing of the genomic DNA from the P544 lethal line showed that ~25 kb of genomic DNA between the original insertion site of the 2487 P element and ~320 bp relative to the transcription initiation site of *D-mef2* had been deleted from the P544 chromosome such that the proximal end of the 2487 P element was inserted in the *D-mef2* promoter. Although it is possible that the P544 chromosome has other nearby alterations, this is unlikely because it is lethal in trans to several recently identified EMS alleles of *D-mef2* (22).
  22. G. Ranganayakulu and R. Schulz, unpublished results.
  23. D. P. Kiehart and R. Feghali, *J. Cell Biol.* **103**, 1517 (1986).
  24. E. Shishido, S.-I. Higashijima, Y. Emori, K. Saigo, *Development* **117**, 751 (1993).
  25. R. Bodmer, *ibid.* **118**, 719 (1993).
  26. N. Azpiazu and M. Frasch, *Genes Dev.* **7**, 1325 (1993).
  27. N. Patel, P. M. Snow, C. S. Goodman, *Cell* **48**, 975 (1987).
  28. A. M. Michelson *et al.*, *Genes Dev.* **4**, 2086 (1990); B. M. Paterson *et al.*, *Proc. Natl. Acad. Sci. U.S.A.* **88**, 3782 (1991).
  29. C. Bourgouin, S. E. Lungren, J. B. Thomas, *Neuron* **9**, 549 (1992); B. Cohen, M. E. McGuffin, C. Pfeifle, D. Segal, S. M. Cohen, *Genes Dev.* **6**, 715 (1992).
  30. C. Dohmann, N. Azpiazu, M. Frasch, *Genes Dev.* **4**, 2098 (1990).
  31. G. Vachon *et al.*, *Cell* **71**, 437 (1992).
  32. J. Sambrook, E. F. Fritsch, T. Maniatis, Eds., in *Molecular Cloning: A Laboratory Manual* (Cold Spring Harbor Laboratory, Cold Spring Harbor, NY, ed. 2, 1989).
  33. The PCR procedure was carried out as described [K. Kaiser and S. F. Goodwin, *Proc. Natl. Acad. Sci. U.S.A.* **87**, 1686 (1990)], with 1/50th of a fly equivalent for each reaction. The primers were P, 5'-CGACGGGACCACCTTATGTTATTCA; A, 5'-GGGATGTCAGGTGCGTGGCGAGGTG; and B, 5'-CCAAAGCGATGTTAGCAGGGGTG. The *D-mef2* insertion line *P[lacZ,ry+J544/CyO* was confirmed by flanking primer sets and by Southern blot analysis.
  34. Embryos were stained with the indicated antibodies as described (31). Antibody dilutions were as follows: anti-D-MEF2, 1:1000; antibody to *Drosophila* muscle myosin (23), 1:400; and anti-Fas-III (provided by C. Goodman) (27), 1:10. For mutant analysis, embryos were double-stained with either anti-D-MEF2 or anti- $\beta$ -galactosidase (Cappell) at a dilution of 1:5000, to identify homozygous mutants. The *CyO* balancer chromosome was marked with an *Antp-lacZ* reporter (obtained from J. Botas), allowing identification of heterozygous embryos from homozygous embryos.
  35. Rabbits were immunized with a histidine-tagged D-MEF2 fusion protein encompassing amino acids 1 to 472 of D-MEF2, cloned in-frame into the pR-SETB vector (Invitrogen). The fusion protein was purified from BL21-LysS cells with the 6XHis/Ni-NTA purification system (Qiagen, Chatsworth, CA).
  36. Within the coding region, introns are found at the following positions: intron 2, after codon 18; intron 3, after codon 86; intron 4, after codon 193; intron 5, after codon 226; intron 6, after codon 329; intron 7, after codon 468. The DNA sequence has been deposited in GenBank, accession number U19493.
  37. The breakpoints of the different deficiency chromosomes were determined by Southern blot analysis with several probes from the *D-mef2* gene and 5' flanking region and from the P element.
  38. Embryos were collected, fixed, and hybridized with digoxigenin-labeled probes (Boehringer-Mannheim), as described previously (10). To identify *D-mef2* homozygous mutants, we double-stained embryos for lacZ activity or *D-mef2* mRNA in parallel with the individual probes. Probes were obtained from the following sources: Dmyd/nautilus (28), apterous (J. Botas), tinman (25), bagpipe (26), S59 (30), and DFR1 (24).
  39. We are grateful to E. McGuffin and W. Mattox for advice and assistance, S. Galewsky for comments on the genetic screen, R. Davis for the gift of the P2487 stock, and D. Kiehart for anti-MHC. We also thank J. Botas for advice. Supported by grants from NIH, the Muscular Dystrophy Association, the Robert A. Welch Foundation (to E.N.O.), and NSF (to R.A.S.) B.L. was supported by an NIH training grant.

2 November 1994; accepted 5 January 1995

## The Functional Significance of Arm Movements in Neonates

A. L. H. van der Meer,\* F. R. van der Weel, D. N. Lee

Arm movements made by newborn babies are usually dismissed as unintentional, purposeless, or reflexive. Spontaneous arm-waving movements were recorded while newborns lay supine facing to one side. They were allowed to see only the arm they were facing, only the opposite arm on a video monitor, or neither arm. Small forces pulled on their wrists in the direction of the toes. The babies opposed the perturbing force so as to keep an arm up and moving normally, but only when they could see the arm, either directly or on the video monitor. The findings indicate that newborns can purposely control their arm movements in the face of external forces and that development of visual control of arm movement is underway soon after birth.

Moving a limb or the whole body in a controlled manner requires acting in conjunction with gravity and other external forces (1). This means that movements cannot be represented in any preprogrammed, context-insensitive way (2). Accurate control requires on-line regulation of muscular activation on the basis of perceptual information about the dynamics of the limb movement and the external force field, as well as about the movement of the limb relative to objects or surfaces to which it is being guided. Are neonates capable of such perceptuo-motor control, or are their movements to be seen as simply reflexive, show-

ing no evidence of intentionality or control?

To test whether newborn babies between 10 and 24 days take account of external gravitational forces in moving their limbs, we measured spontaneous arm-waving movements while the baby lay on its back with its head turned to one side (3). Free-hanging weights, attached to each wrist by strings passing over pulleys, pulled on the arms in the direction of the toes (Fig. 1A). The hand the baby was facing was called the ipsilateral hand; the opposite hand was called the contralateral hand (Fig. 1B).

A typical recording of a newborn baby waving both arms with no weights attached is shown in Fig. 1C. The seen ipsilateral hand shows much movement, whereas the unseen contralateral hand is predominantly stationary with only occasional movement. To test whether newborns need to see their

Perception in Action Laboratories, Department of Psychology, University of Edinburgh, 7 George Square, Edinburgh EH8 9JZ, UK.

\*To whom correspondence should be addressed.